Comparison of Column Water Vapor Measurements Using Downward-looking Near-Infrared and Infrared Imaging Systems and Upward-looking Microwave Radiometers

BO-CAI GAO,* ED R. WESTWATER,† B. BOBA STANKOV,† D. BIRKENHEUER,‡# AND ALEXANDER F. H. GOETZ*

*Center for the Study of Earth from Space, University of Colorado, Boulder, Colorado
†NOAA/ERL Wave Propagation Laboratory, Boulder, Colorado
‡Cooperative Institute for Research in the Atmosphere, Fort Collins, Colorado
#NOAA/ERL Forest System Laboratory, Boulder, Colorado

(Manuscript received 6 May 1991, in final form 18 February 1992)

ABSTRACT

Remote soundings of precipitable water vapor from three systems are compared with each other and with ground truth from radiosondes. Ancillary data from a mesoscale network of surface observing stations and from wind-profiling radars are also used in the analysis. The three remote-sounding techniques are: (a) a reflectance technique using spectral data collected by the Airborne Visible–Infrared Imaging Spectrometer (AVIRIS); (b) an emission technique using Visible–Infrared Spin Scan Radiometer (VISSR) Atmospheric Sounder (VAS) data acquired from the National Oceanic and Atmospheric Administration's (NOAA) Geostationary Operational Environmental Satellite (GOES); and (c) a microwave technique using data from a limited network of three ground-based dual-channel microwave radiometers. The data were taken over the Front Range of eastern Colorado on 22–23 March 1990. The generally small differences between the three types of remote-sounding measurements are consistent with the horizontal and temporal resolutions of the instruments. The microwave and optical reflectance measurements agreed to within 0.1 cm; comparisons of the microwave data with radiosondes were also either that good or explainable. The largest differences between the VAS and the microwave radiometer at Elbert were between 0.4 and 0.5 cm and appear to be due to variable terrain within the satellite footprint.

1. Introduction

Water vapor is difficult to measure and analyze because of a number of factors, including a high degree of horizontal, vertical, and temporal variation (Liebe 1980); a large range of variation; and the adverse effects of clouds on remote sensing (Starr and Melfi 1991). Although it would be highly desirable to measure with good temporal resolution both the vertical and horizontal profiles of vapor, measurements of the integrated water vapor content from ground to space are useful for some applications. Such applications include meteorology, climate, radiative transfer, and radio interferometry. Starr and Melfi (1991) have recently stressed that "the value of even a relatively gross description of atmospheric water vapor is extremely high at this time." In this paper, we compare three techniques for measuring the integrated water vapor content, which is also referred to as column water vapor amount or as precipitable water vapor (PWV).

A technique referred to as the reflectance technique in this paper can be used to derive column water vapor amounts (Gao and Goetz 1990) from spectral data collected by the Airborne Visible–Infrared Imaging Spectrometer (AVIRIS) (Vane 1987). AVIRIS measures the solar radiation that is reflected by the earth's surface at high spatial and spectral resolution from a high-altitude aircraft.

Column water vapor retrievals over land areas from satellite IR emission measurements using, for example, the split-window technique (Chesters et al. 1983) are possible during clear conditions. Other works on satellite infrared emission retrievals of precipitable water vapor include Kleespies and McMillin (1990) and Smith et al. (1985). Spatial resolutions using these techniques range from 8 to 50 km.

Both the column water vapor and cloud liquid water can be obtained from emission measurements made with ground-based microwave radiometers (Hogg et al. 1983a). The advantages of this technique are that (a) it provides data during cloudy conditions and light rain, and (b) it provides continuous time series with measurements from unattended instruments. Information on the temporal variability of water vapor, as derived from microwave radiometers, has been published by Hogg et al. (1981), Ciotti et al. (1987), and Rogers and Schwartz (1991).

This paper compares water vapor measurements taken in the Front Range of eastern Colorado during

Corresponding author address: Dr. Bo-Cai Gao, University of Colorado, CIRES, Campus Box 449, Boulder, CO 80309-0449.

clear conditions using the three techniques: the reflectance technique, an infrared emission technique applied to geostationary satellite measurements, and the microwave technique. Ancillary data from radiosondes, a network of surface observations, and wind profilers are also used in this comparison. As will be shown, the measurements of the optical technique, the microwave technique applied to ground-based measurements, and radiosondes generally agree to within 0.1 cm.

2. Techniques used for water vapor measurements

a. Imaging spectrometers: The optical reflectance technique

Imaging spectrometers acquire images in hundreds of contiguous spectral bands such that for each picture element (pixel), a complete reflectance or emittance spectrum can be derived from the wavelength region covered (Goetz et al. 1985). In the coming decade, the National Aeronautics and Space Administration (NASA) expects to carry the High-Resolution Imaging Spectrometer (HIRIS) (Goetz and Herring 1989) aboard a polar platform of the Earth Observation System (EOS). The precursor to HIRIS is AVIRIS, which is now operational. AVIRIS images the earth's surface in 224 spectral bands, each approximately 10 nm wide, covering the region 0.4–2.5 μm, from an ER-2 aircraft at an altitude of 20 km; the ground instantaneous field of view is 20 $\times$ 20 m^2. Figure 1a shows the AVIRIS observational geometry, and Fig. 1b shows an example of an AVIRIS spectrum. The water vapor absorption features (minima) centered at approximately 0.94, 1.14, 1.38, and 1.88 μm are clearly visible. The 0.94- and 1.14-μm bands are useful for water vapor retrievals from AVIRIS data. However, the 1.38- and 1.88-μm bands are saturated under typical atmospheric conditions and are less useful for quantitative retrievals.

A technique for water vapor retrievals from AVIRIS data was described by Gao and Goetz (1990). In this technique, the quantitative retrieval is made by curve fitting AVIRIS spectra with calculated spectra in the 0.94- and 1.14-μm water vapor band absorption regions using an atmospheric transmission model, a narrow-band spectral model, and a nonlinear least-squares fitting technique. The derivation used the facts that 1) the reflectances of many ground targets vary approximately linearly with wavelength in the 0.94- and 1.14-μm water vapor band absorption regions, 2) the scattered radiation near 1 μm is small compared with the directly reflected radiation when the atmospheric aerosol concentrations are low, and 3) the scattered radiation in the lower part of the atmosphere is subjected to the water vapor absorption. The technique is directly applicable for retrieving column water vapor amounts from AVIRIS spectra measured on clear days with visibilities of 20 km or greater. The precision of the retrieved column water vapor amounts is approximately 3%. Figure 2 shows an example of spectral curve fitting. During the fitting process, the water vapor value and the spectral background—a linear function of wavelength—are allowed to vary. The best estimate of the water vapor value and the spectral background are obtained when the sum of the squared differences between the observed and the calculated spectra is minimized. Discussions on the nonlinearity of surface reflectances in the 0.94- and 1.14-μm water vapor band absorption regions have been presented by Gao and Goetz (1990).

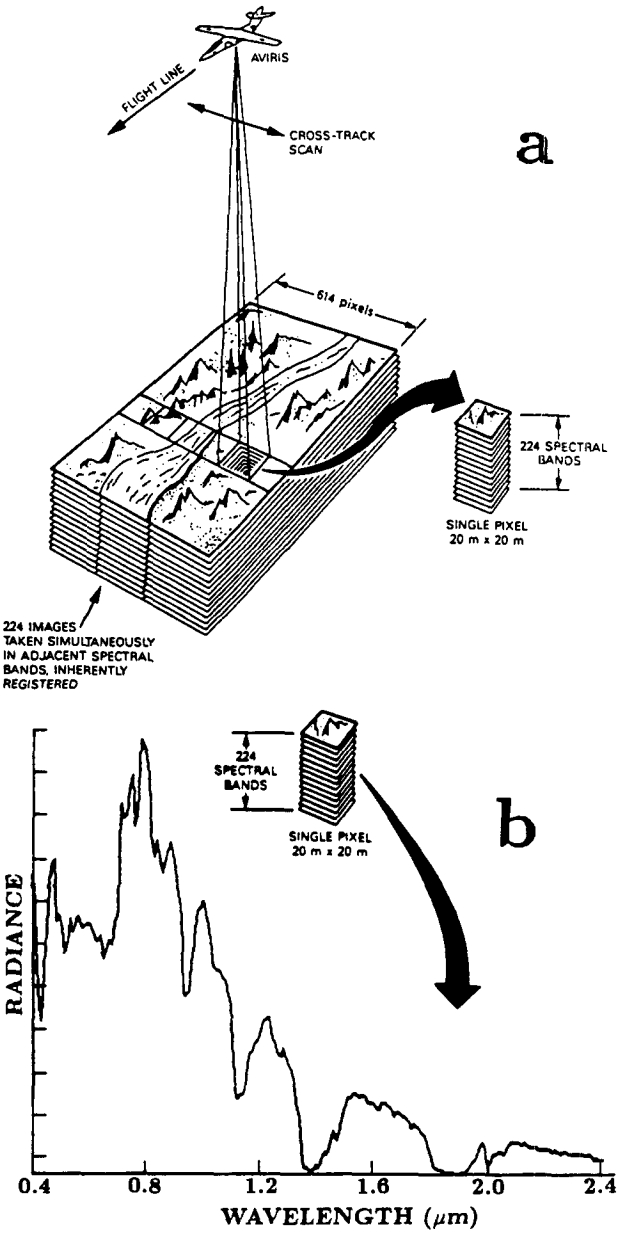

FIG. 1. (a) AVIRIS data collection geometry and (b) a spectrum from a single AVIRIS pixel (Vane 1987).

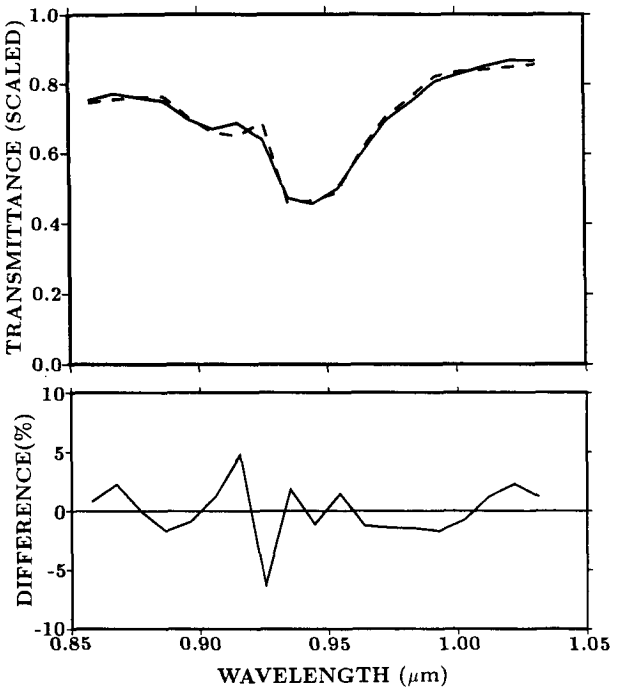

FIG. 2. An example of curve fitting of spectra. The top plot shows the observed spectrum (solid curve) and the fitted spectrum (dashed curve). The bottom plot shows the percentage differences between the observed and the fitted spectra.

Because atmospheric scattering is not modeled explicitly, our retrieving technique is not directly applicable for deriving water vapor values from AVIRIS data measured on hazy days. The scattering effect must be included in atmospheric radiative transfer models when deriving column water vapor values from AVIRIS data measured on hazy days. Uncertainties in the amount of aerosol and aerosol vertical distribution also introduce errors in derived column water vapor values.

The solar radiation near 1 μm is mostly reflected at the top portions of low-level water clouds. The column water vapor amounts between the ground and the top of the atmosphere cannot be obtained from AVIRIS data over these clouds. However, the amounts of water vapor above these clouds can be obtained from the AVIRIS data.

b. *Quantitative PWV spatial analyses from LAPS–VAS*

The National Oceanic and Atmospheric Administration's (NOAA) Geostationary Operational Environmental Satellite (GOES) offers real-time data from the Visible–Infrared Spin Scan Radiometer (VISSR) Atmospheric Sounder (VAS). The data contain infrared radiances in 12 spectral bands ranging from 3 to 12 μm. Three channels are water vapor sensitive, seven channels are temperature sensitive, and two window channels are for cloud and skin-temperature measurements. The data are ingested by the NOAA Forecast Systems Laboratory (FSL). Depending on the channel resolution, the data represent fields of view of either 8×8 or 16×16 km^2.

FSL uses a technique by Birkenheuer (1991) to derive a PWV field on a local scale supporting its local analysis and prediction system (LAPS). The analysis requires several (typically 20–50) VAS temperature–moisture soundings in a domain covering a multistate region that includes the LAPS domain. The soundings are produced from the physical VAS sounding retrieval algorithm developed at the University of Wisconsin at Madison (Hayden 1988). Following this, each of these dewpoint temperature soundings is integrated to establish a set of precipitable-water "values." These values are then regressed with the available collocated VAS channel brightness temperatures (the same dwell-sounding data that were used in the physical retrieval algorithm). Next, the VAS brightness-temperature fields are made continuous by replicating and smoothing the data; details are explained in Birkenheuer (1991). The regression coefficients relating channel brightness to precipitable water are then applied to the continuous VAS brightness temperatures to yield a PWV scene centered over the Rocky Mountain foothills extending outward 300 km in each direction. Values for cloudy areas are determined using interpolation. The field is used to assign values to the 10-km LAPS grid. A final analysis step corrects the bias error by raising or lowering the entire field by a constant determined by fitting the field to data from the dual-channel microwave radiometers. In this step, microwave data are only used if clear conditions exist over the radiometers. Thus, a PWV field from VAS with bias corrections based on millimeter-wave radiometer measurements is obtained. This end product is referred to as the PWV analysis data. PWV analyses combine the gradient information from the VAS field with better calibrated ground-based radiometer data, yielding a superior analysis than could be obtained separately from either data source.

The clear advantage of the method is its potential to provide frequent horizontal PWV analyses with local-scale resolution. With a few ground-based PWV data, it is possible to align the PWV analysis and perceive the spatial detail in the field between the ground-based data sites. The technique's chief disadvantage is cloudiness, which can interfere to such a large degree that an analysis not possible.

c. *Dual-channel microwave radiometers: The microwave technique*

The Wave Propagation Laboratory (WPL) of NOAA operates a limited network of dual-channel microwave radiometers (Westwater and Snider 1989). The first

radiometer of this network was installed in 1979; three others were operated between 1985 and 1988. Currently, radiometers are routinely operated at Stapleton International Airport in Denver, Colorado, and at Platteville, Colorado (about 50 km north of Denver); two other instruments are deployed for special projects. In this paper, data from radiometers at Denver, Platteville, and Elbert, a station in Colorado about 70 km south of Denver, were used. These instruments measure downwelling atmospheric thermal emission in the zenith direction at a water vapor–sensitive frequency (20.6 GHz) and a cloud-liquid–sensitive frequency (31.65 GHz). From measurements at the two frequencies, precipitable water vapor and integrated cloud liquid are derived. Details of the instruments and their accuracies were discussed by Hogg et al. (1983b). On the basis of one year's data, the difference between the PWV measurements by the radiometer and those obtained from National Weather Service (NWS) radiosondes is 0.17 cm rms (Hogg et al. 1983a). Operationally, the data are available every 2 min except during precipitation.

d. Radiosondes

In our attempts to obtain ground truth for the remote-sensing measurements, two types of radiosonde systems were used. The first, deployed by NWS, uses standard VIZ ACCU-LOK humidity sensors. The second, deployed by the National Center for Atmospheric Research (NCAR), uses HUMICAP humidity sensors in the CLASS (Cross-chain Loran Atmospheric Sounding System). Studies of the "functional precision" of NWS radiosondes by Hoehne (1980) lead to an uncertainty in PWV of about 0.11 cm rms. A study of the differences between the NWS and CLASS systems was conducted by Wade and Wolfe (1989). They showed that substantial differences between the two systems can occur when the relative humidity is less than 20%. In another experiment of only one week duration, NWS and CLASS sensors were compared with each other (rms difference = 0.07 cm), and the difference between the microwave radiometer and CLASS was 0.04 cm rms (Smith et al. 1990).

3. Results

a. Imaging spectrometer data

AVIRIS data were acquired over the Denver–Platteville area and then over an area east of Greeley, Colorado, about 1940 UTC 22 March 1990. When the AVIRIS measurements were made, the sky was clear and the surface visibility was greater than 50 km. Figure 3a shows a 0.86-μm image of the Denver–Platteville area. The AVIRIS radiances were averaged spatially on a 2-pixel × 2-pixel basis when the image was produced. The spatial averaging was necessary because of the limitation of our image-processing hardware. The Denver Stapleton International Airport is at the lower left part of the image; Platteville is at the upper part. Highway 85, which connects Denver and Platteville, is seen as a curved line. The image covers a surface area of approximately 11×68 km^2.

Column water vapor amounts were retrieved by curve fitting the 0.94-μm water vapor band. The signal-to-noise ratios are approximately 60 for channels near the center of the 0.94-μm water vapor band and 100 for channels in the nearby atmospheric windows. The AVIRIS data were averaged spatially on a 4-pixel × 4-pixel basis to decrease the computer time. The spatial averaging also increases the signal-to-noise ratios by a factor of 4. The retrieval took approximately 25 h on a Microvax III computer. Low vertical resolution temperature, pressure, and water vapor volume mixing-ratio profiles measured near the airport by a six-channel microwave radiometer (Hogg et al. 1983b) were used in the spectral calculations during the curve-fitting process. Figure 3b shows an image processed from the retrieved column water vapor values. To produce a water vapor image having the same size as the image in Fig. 3a, the retrieved water vapor values were zoomed spatially on a 2-pixel × 2-pixel basis. The narrow vertical bar on the right side of Fig. 3b gives the scale of water vapor values from 0.53 cm (blue) to 0.76 cm (red), a very small range. Larger-scale features are also obvious in Figure 3b. From the airport to Platteville, the image shows a blue–red–blue–red variation pattern. The column water vapor values in the entire scene had a mean of 0.640 cm and a standard deviation of 0.044 cm. The horizontal lines in Fig. 3b are artifacts and are due to errors in the AVIRIS radiometric calibration. A few column water vapor values were also derived by curve fitting the 1.14-μm water vapor band. These values were systematically different from those obtained by curve fitting the 0.94-μm band by approximately 6%. In order to test the sensitivity of water vapor retrievals to the assumed atmospheric models, a number of water vapor values were derived by using the midlatitude summer atmospheric model from LOWTRAN6 (Kneizys et al. 1983). The results only differed by 0.62% from those using the temperature, pressure, and water vapor volume mixing-ratio profiles measured with the six-channel microwave radiometer. The small difference indicates the insensitivity of water vapor retrievals to the assumed atmospheric models.

A topographic map of the AVIRIS scene is shown in Fig. 3c. Generally, the surface elevation decreases monotonically from the airport area ($\sim$1630 m) to Platteville ($\sim$1450 m). Small variations of surface elevation in the east–west direction are also present. Column water vapor amount usually decreases as the surface altitude increases because atmospheric water vapor concentration decreases rapidly with height. Therefore, the column water vapor amount from the airport to Platteville was expected to increase monotonically. The

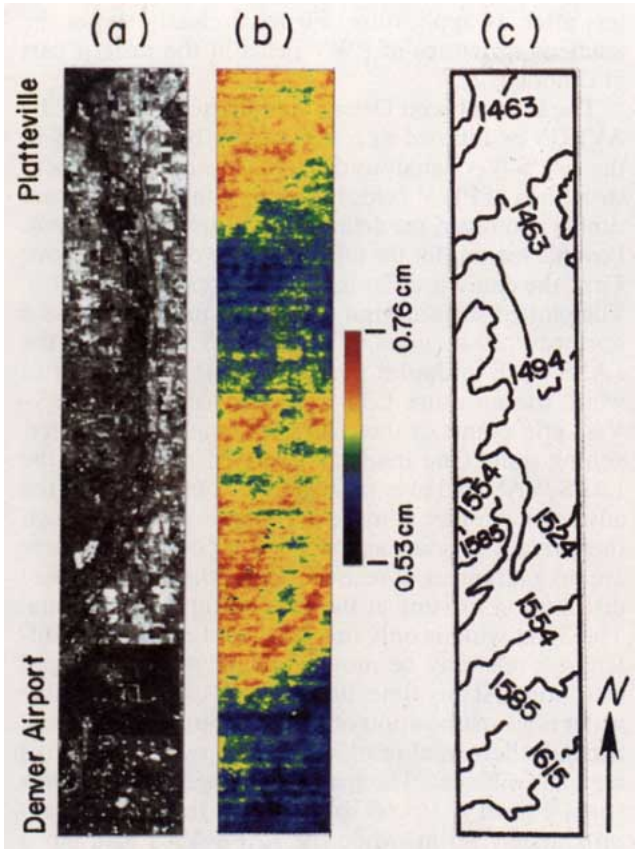

FIG. 3. Column water vapor retrievals from AVIRIS data measured over the Denver–Platteville area in Colorado on 22 March 1990: (a) an image of the scene processed from radiances of one channel centered at 0.86 μm, (b) a column water vapor image over the scene retrieved by curve fitting the 0.94-μm water vapor band absorption region, and (c) a topographic map of the scene. The elevations in the topographic map are in meters. The distance from left to right of the images is approximately 11 km.

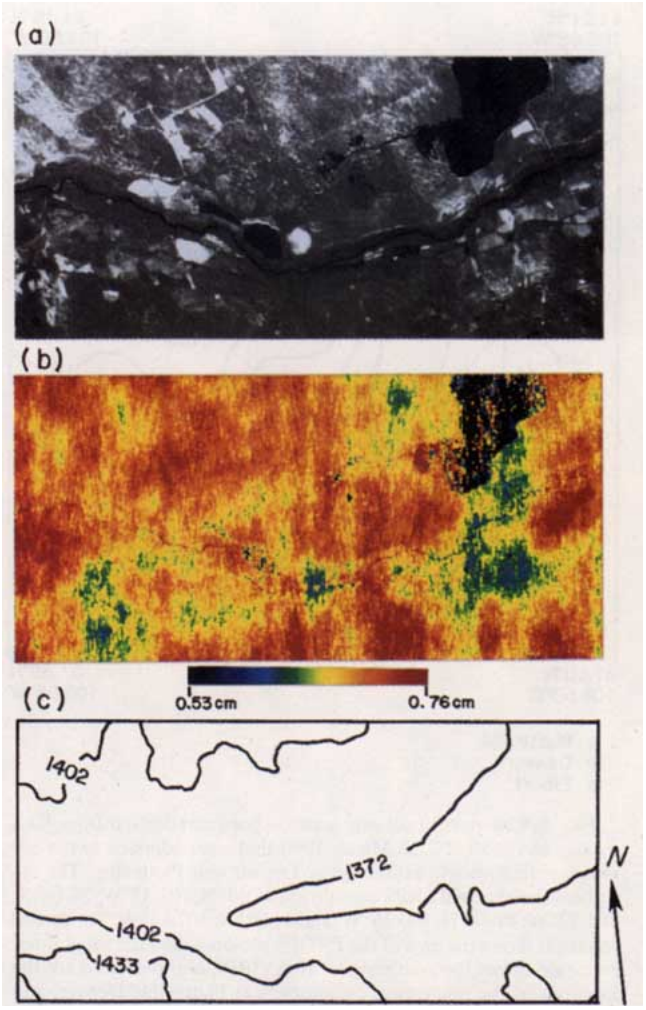

FIG. 4. Column water vapor retrievals from AVIRIS data measured over an area east of Greeley, Colorado, on 22 March 1990: (a) an image of the scene processed from radiances of one channel centered at 0.86 μm, (b) a column water vapor image over the scene, retrieved by curve fitting the 0.94-μm water vapor band absorption region, and (c) a topographic map of the scene. The elevations and distances are as in Fig. 3.

observation of a blue–red–blue–red pattern from the bottom to the top in Fig. 3b indicated that real spatial variations of water vapor distributions, not entirely related to the topographic effects, existed when the AVIRIS data were acquired. The observed spatial variation of column water vapor amount on the order of 0.1 cm indicates the high precision with which column water vapor amounts can be determined from AVIRIS data.

Figures 4a, 4b, and 4c are similar to Figs. 3a, 3b, and 3c, respectively, except that the data were acquired over an area east of Greeley. Figure 4c shows that there are surface-elevation variations of approximately 60 m within the scene. The column water vapor values in the entire scene had a mean of 0.686 cm and a standard deviation of 0.049 cm. Figure 4b also shows spatial variations of column water vapor amounts that are not related to the topographic effects. The derived water vapor values over the lake are smaller than those over the solid surface areas. This may be due to the lower signal-to-noise ratio of the AVIRIS data over the lake, where the surface reflectances are less than 5%. This may also be due to the fact that the atmospheric transmission model used in our retrievals is not sufficient to model the spectra over the low-reflectance lake, where large portions of the observed radiances result from the single scattering by atmospheric aerosols.

b. LAPS–VAS PWV analysis data

LAPS–VAS PWV analysis data for both Platteville and Denver were obtained for 1245, 1545, and 1845 UTC; data for the last case are plotted in Fig. 5. An automated cloud-detection algorithm classified all three scenes as clear within a 20-km radius of each radiometer; hence, both the Denver and Platteville radi-

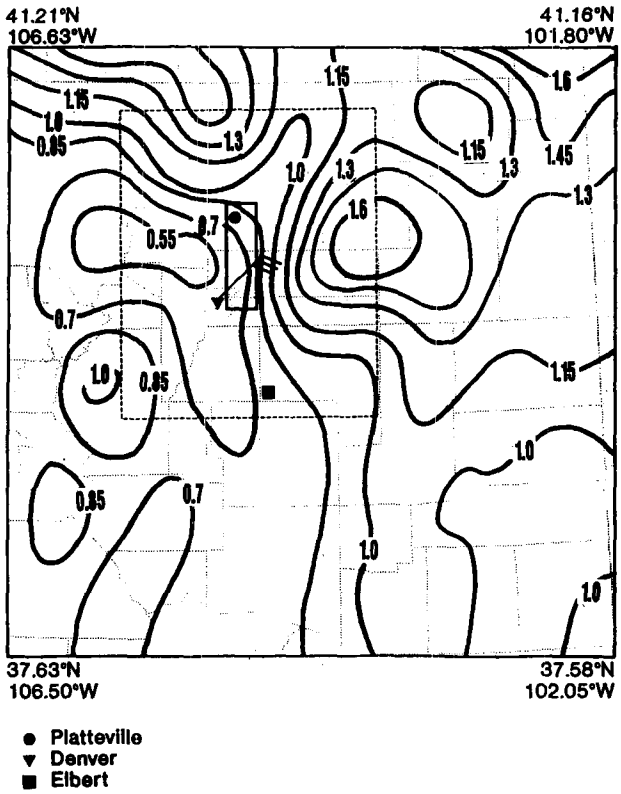

FIG. 5. Contours of column water vapor (cm) derived from VAS images at 1845 UTC 22 March 1990 that were adjusted to the microwave radiometric soundings at Denver and Platteville. The coordinates of the total LAPS domain are 36.90°N, 107.35°W; 36.83°N, 101.22°W; 41.84°N, 100.76°W; and 41.91°N, 107.64°W. The dashed rectangle shows the area of the PROFS mesonet, and the small inner rectangle shows the area imaged by AVIRIS; also indicated are the locations of the microwave radiometers at Platteville, Denver, and Elbert. The wind barb out of Denver shows the direction and magnitude of the surface winds at Denver. The contour interval for column water vapor is 0.15 cm.

ometers were used to determine a field bias. The bias correction algorithm used differences between the initial LAPS–VAS field and the radiometers to determine discrete radiometer bias corrections (the amount to be added or subtracted to the LAPS–VAS field to make it agree with the radiometer). A total field bias correction for each time period was then determined from a weighted average of the discrete bias correction terms. The discrete bias corrections are weighted inversely with respect to the LAPS–VAS horizontal moisture gradient (first derivative) over each radiometer. Weighting in this manner reduces the effects of misnavigated satellite data, favoring the discrete bias correction term in a region where translating the LAPS–VAS field in any direction would have less impact. Bias errors for 1245, 1545, and 1845 UTC were −0.2542, +0.2252, and +0.2339 cm of PWV for each respective time period. The determined bias correction worked well because it agreed well with both radiometers after its application. Figure 5 clearly shows the gradient structures of PWV fields in the eastern part of Colorado.

The area between Denver and Platteville imaged by AVIRIS is outlined as a rectangular box in Fig. 5 in the LAPS–VAS analysis domain. The overall gradient structures of PWV fields in this box and in Fig. 3b are similar; however, the detailed PWV fields are different. Possible reasons for the differences are described below. First, the datasets differ in time by approximately 1 h. The plotted surface wind in the field in Fig. 5 shows a northeast 30-kt wind. The AVIRIS track and the LAPS–VAS gridpoint spacing are 10 km. With this wind, the moisture field would advect three LAPS–VAS grid points or three AVIRIS swaths in the intervening time. One might be tempted to translate the LAPS–VAS field over the region to compensate for the advection in order to make a comparison. Even though there might be some agreement after doing this, there are no guarantees of reconstructing the true moisture distribution existing at the time of the AVIRIS data. The 30-kt wind is only one level, and moisture at different levels may be moving at different speeds and directions. At any time, the observed total precipitable water is a superposition of the water vapor at all levels. Second, the spatial resolution of the two data sources are quite different. The spatially averaged AVIRIS data (on a 4-pixel × 4-pixel basis) have a resolution of approximately 80 m, while the LAPS–VAS field has a spatial resolution of approximately 30 km (Birkenheuer 1991). The 10-km LAPS–VAS fields will never show the level of detail available with AVIRIS. Also, since the AVIRIS data cover a narrow region, there is no way with this case to sufficiently average the AVIRIS water vapor to correspond to the LAPS–VAS resolution.

c. *The microwave technique and radiosondes*

Eighteen-hour segments of data at three locations were chosen to compare the PWV retrievals of the microwave radiometers with other types of PWV data. Figure 6 shows 2-min time series of radiometer data at Platteville, Denver, and Elbert. The three radiometers were being operated as a part of the Winter Icing and Storms Project (WISP90) (Stankov et al. 1990). The figure also shows the NWS synoptic soundings at 1100 and 2300 UTC 22 March at Denver; soundings from special releases of CLASS radiosondes at 0000 and 0300 UTC 23 March at Elbert; adjusted VAS PWV soundings at Platteville, Denver, and Elbert; and two optical reflectance soundings at Denver and Platteville near 1940 UTC 22 March. As discussed in sections 2b and 3a, the VAS soundings are not independent of the microwave ones at Denver and Platteville; however, for all practical purposes, PWV derived by the reflectance technique is completely independent. Except for the three VAS soundings at Elbert (see section 3d) and

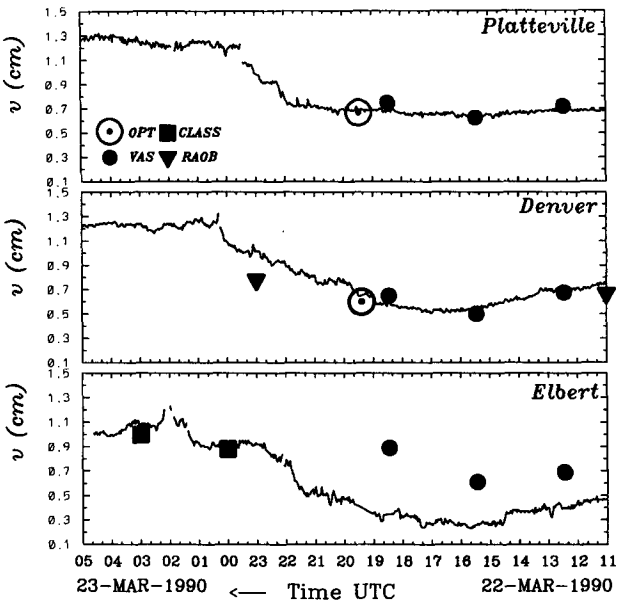

FIG. 6. Time series of precipitable water vapor. Continuous curves are from microwave radiometers, rectangles from CLASS radiosondes, triangles from NWS radiosondes, dark circles from VAS-adjusted images, and open circles from aircraft measurements that used the optical reflectance technique.

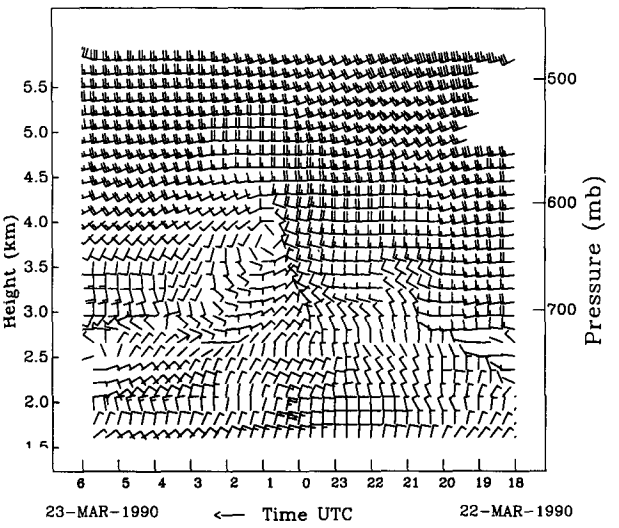

FIG. 7. Wind velocity 20-min profiles measured by the 915-MHz Stapleton wind profiler between 1800 UTC 22 March and 0600 UTC 23 March 1990. Wind flag = 25 m s^{-1}, barb = 5 m s^{-1}, half-barb = 2.5 m s^{-1}. Ground level is at 1611 m.

the NWS sounding at 2300 UTC, all soundings were in excellent agreement. The difference of more than 0.2 cm between the radiometer data and the data from NWS radiosonde at 2300 UTC requires further explanation. Evidence is presented in section 3d to support our conclusion that this difference was due to the NWS balloon moving into a region of dry air, and hence did not reflect the buildup of moisture that was observed during this time by all three radiometers. That a buildup was occurring was also supported by the two special CLASS releases at Elbert at 0000 and 0300 UTC 23 March. This increase in moisture was followed by a well-documented event of supercooled liquid water that lasted for three days (Stankov et al. 1990).

d. Meteorological situation during the remote-sensor observations

The AVIRIS flight took place in the warm, dry air during the 6 h before a cold front associated with a high pressure cell over Montana was pushed southwestward through the Front Range area. The temperature behind the front was −8°C. Figure 7 shows 20-min wind profiles from the Denver 915-MHz wind profiler and surface winds from the PROFS (Program for Regional Observing and Forecasting Systems) mesonet station at Aurora (near the Denver airport), Colorado, between 1800 UTC 22 March and 0600 UTC 23 March 1990. The onset of stronger northerlies at 0000 UTC 23 March was associated with the frontal passage. Figure 8 shows the analysis of the PROFS mesonet surface data for 0000 UTC 23 March. Heavy solid lines represent the surface absolute humidity. Strong surface winds of 25–45 km behind the front

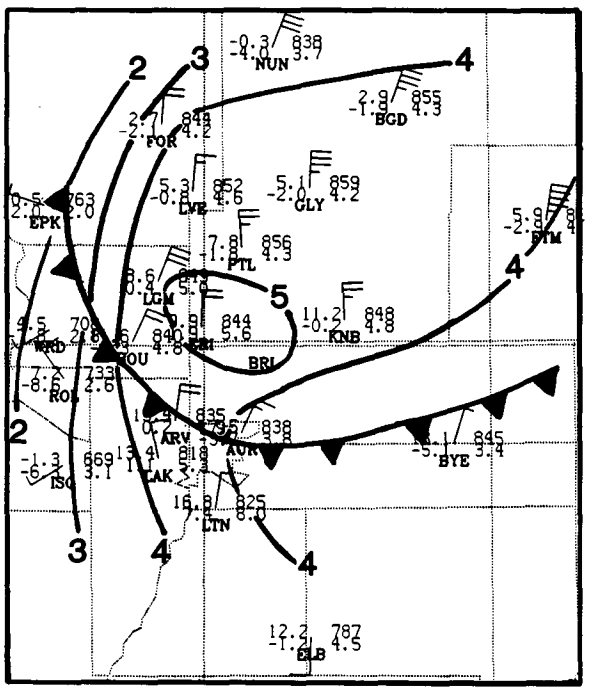

FIG. 8. Mesonet data analysis. Heavy solid lines are surface absolute humidity (g m^{-3}) at 0000 UTC 23 March 1990. The four numbers around each station are temperature (°C, top left), dewpoint temperature (°C, bottom left), surface pressure (hPa, top right), and absolute humidity (g m^{-3}, bottom right). Heavy triangles indicate the position of the cold front.

brought the cold, moister air into the Front Range region. However, the Denver radiosonde released at 2300 UTC 22 March would have been carried by the northerly surface flow into the drier air southward. From Fig. 7, we see that the northerly flow persisted up to 3.0 km MSL, thus providing a strong push of the radiosonde toward the dry air throughout the first 2 km of its ascent. The NWS surface absolute humidity data analysis (not shown here) also reveals a large area of dry air covering southern Colorado, Arizona, and New Mexico.

4. Discussion

The measurement comparisons clearly illustrate the difficulty of verifying remotely sensed water vapor. In our particular case, much time was spent in determining the reasons for the discrepancy between the radiometer's and NWS radiosonde's sounding of water vapor on 2300 UTC 22 March. Figure 6 showed that all three radiometers at Denver, Platteville, and Elbert indicated a consistent increase in PWV after about 2100 UTC. Since the radiometers are independent systems, it was apparent that the problem was the nonrepresentativeness of the radiosonde data; that is, the winds blew the balloon into a drier region than that above the Stapleton radiometer. However, without the existence of data from the other two radiometers, such a difference might easily have been attributed to a radiometric calibration error.

The advantage of the LAPS–VAS analysis is purported to be its spatial coherence. Point data sources, such as the ground-based radiometers, do not show changes in the PWV field at resolutions smaller than that determined by their geographical locations. The LAPS–VAS analysis ostensibly gives detail of this structure. Both the Elbert data and aircraft data were made available in this study much after the real-time LAPS–VAS analyses were generated. Therefore, comparison of the LAPS–VAS PWV analysis with both sources constitutes independent appraisals of the LAPS–VAS technique.

The LAPS–VAS values in Fig. 6 for PWV at Elbert at the three times (1245, 1545, and 1845 UTC) were obtained directly from analysis plots such as Fig. 5. As mentioned earlier, LAPS–VAS PWV data are bias corrected using only data from Platteville and Denver radiometers. Comparing LAPS–VAS data to the Elbert radiometer data is a blind test of the LAPS–VAS PWV analysis. Figure 6 shows that the LAPS–VAS analysis reported a consistently higher level of PWV in this area. Moreover, the difference at 1845 UTC is slightly greater than the differences of the preceding time periods.

The slightly greater difference at 1845 UTC may be explainable. We can assume that Elbert was on the dry side of the PWV boundary at 1845 UTC. This is supported by the trend in the Elbert radiometer data, placing Elbert in the dry regime at that time, and by the LAPS–VAS field that suggests the moisture gradient was very near the region with higher readings to the east and north. With the prevailing northeasterly winds (Fig. 7), the moisture was poised to advect over Elbert near the time of this analysis. The resolution of the LAPS–VAS analysis, which has a grid spacing of 10 km, is roughly 30 km. Therefore, moisture discontinuities on smaller scales will suffer degradation. The moisture boundary close to Elbert was probably "blurred" by the analysis, causing the PWV values on the dry side of the boundary to increase and values on the moist side of the boundary to decrease with respect to truth. This argument (resolution limitation) could possibly explain the regular differences between the LAPS–VAS and Elbert radiometer data at 1245, 1545, and 1845 UTC.

The differences may also be explained by topographical differences. The radiometer site is in an area of varying terrain. The atmosphere over higher terrain usually contains less moisture than the atmosphere over lower terrain. A possible explanation of the consistent moist bias of the LAPS–VAS in Fig. 6 may be low spatial resolution over an area having highly varying optical depth. The blending of the higher moisture levels at adjacent lower elevations with the water vapor signal over the higher terrain would effectively raise the analyzed amount in a region similar to Elbert.

5. Summary

We compared PWV soundings from the three separate remote-sensing systems: optical reflectance, VAS, and dual-channel microwave radiometers. The microwave measurements were also compared with soundings from both NWS and CLASS radiosondes. The microwave and reflectance measurements agreed to within 0.1 cm, and the comparisons with the radiosondes were also either that good or explainable. The poorest agreement of the systems, roughly 0.4–0.5 cm, was between the microwave and the VAS at a location where topographical influences may be significant. Each of the techniques can provide complementary information of PWV. The reflectance technique provides column water vapor amounts during clear conditions at a precision better than 0.1 cm and at high spatial resolution. The microwave radiometer provides nearly continuous data during both clear and cloudy conditions but only at a limited set of locations. The column water vapor amounts derived from microwave radiometer data can be used to quantitatively adjust satellite PWV images provided by the VAS. The data presented in this paper confirm that atmospheric water vapor is a very complex, highly mobile species and that seemingly straightforward comparisons require great care in interpretation. Although we have focused primarily on comparison of three systems, it is also apparent that their data are complementary and could be blended both temporally and spatially. Data from

such multiple sources will be required to capture significant features of water vapor.

Acknowledgments. We thank J. A. Schroeder for many useful suggestions on the manuscript. R. G. Strauch provided the wind profiler data for Fig. 7. We are also grateful to R. O. Green for providing the AVIRIS spectral data. This work was partially supported by the Jet Propulsion Laboratory, California Institute of Technology, under Contract 958039; the FAA under Contract DTAF01-90-Z-02005; and the Jet Propulsion Laboratory under the auspices of the National Aeronautics and Space Administration (NASA) as a part of the NASA Propagation Program.

REFERENCES

Birkenheuer, D. L., 1991: An algorithm for operational water vapor analyses integrating GOES and dual-channel microwave radiometer data on the local scale. *J. Appl. Meteor.,* **30,** 834–843.

Chesters, D. C., L. W. Uccellini, and W. D. Robinson, 1983: Low-level water vapor fields from the VISSR Atmospheric Sounder (VAS) "split-window" channels. *J. Climate Appl. Meteor.,* **22,** 725–743.

Ciotti, P., E. R. Westwater, M. T. Decker, A. J. Bedard, Jr., and B. B. Stankov, 1987: Ground-based microwave radiometric observations of the temporal variation of atmospheric geopotential height and thickness. *IEEE Trans. Geosci. Electron.,* **GE-25,** 600–615.

Gao, B.-C., and A. F. H. Goetz, 1990: Column atmospheric water vapor and vegetation liquid water retrievals from airborne imaging spectrometer data. *J. Geophys. Res.,* **95,** 3549–3564.

Goetz, A. F. H., and M. Herring, 1989: The high resolution imaging spectrometer (HIRIS) for Eos. *IEEE Trans. Geosci. Remote Sens.,* **27,** 136–144.

——, G. Vane, J. Solomon, and B. N. Rock, 1985: Imaging spectrometry for Earth remote sensing. *Science,* **228,** 1147–1153.

Hayden, C. M., 1988: GOES-VAS simultaneous temperature-moisture retrieval algorithm. *J. Appl. Meteor.,* **27,** 705–733.

Hoehne, W. E., 1980: Precision of National Weather Service upper air measurements. NOAA Tech. Memo. NWS T&ED-16 [NTIS No. PB81-108136], NOAA National Weather Service, Sterling, VA, 23 pp.

Hogg, D. C., F. O. Guiraud, and W. B. Sweezy, 1981: The short-term temporal spectrum of precipitable water vapor. *Science,* **213,** 1112–1113.

——, ——, J. B. Snider, M. T. Decker, and E. R. Westwater, 1983a: A steerable dual-channel microwave radiometer for measurement of water vapor and liquid in the troposphere. *J. Appl. Meteor.,* **22,** 789–806.

——, M. T. Decker, F. O. Guiraud, K. B. Earnshaw, D. A. Merritt, K. P. Moran, W. B. Sweezy, R. G. Strauch, E. R. Westwater, and C. G. Little, 1983b: An automatic profiler for the wind, temperature, and humidity in the atmosphere. *J. Appl. Meteor.,* **22,** 807–831.

Kneizys, F. X., E. P. Shettle, W. O. Gallery, J. H. Chetwynd, L. W. Abreu, J. E. A. Selby, S. A. Clough, and R. W. Fenn, 1983: Atmospheric transmittance/radiance: Computer code LOWTRAN6, 200 pp. [Available from AFGL-TR-83-0187, Air Force Geophys. Lab., Bedford, MA]

Kleespies, T. J., and L. M. McMillin, 1990: Retrieval of precipitable water from observations in the split window over varying surface temperatures. *J. Appl. Meteor.,* **29,** 866–877.

Liebe, H. J., 1980: Atmospheric water vapor: A nemesis for millimeter wave propagation. *Atmospheric Water Vapor,* A. Deepak, T. D. Wilkerson, and L. H. Ruhnke, Eds., Academic, 143–201.

Rogers, R. R., and A. P. Swartz, 1991: Mesoscale fluctuations of columnar water vapor. *J. Appl. Meteor.,* **30,** 1305–1322.

Smith, W. L., G. S. Wade, and H. M. Woolf, 1985: Combined atmospheric sounding/cloud imagery—A new forecast tool. *Bull. Amer. Meteor. Soc.,* **66,** 138–141.

——, H. E. Revercomb, H. B. Howell, H. M. Woolf, R. O. Knuteson, R. G. Decker, M. J. Lynch, E. R. Westwater, R. G. Strauch, K. P. Moran, B. Stankov, M. J. Falls, J. Jordan, M. Jacobsen, W. F. Dabbert, R. McBeth, G. Albright, C. Paneitz, G. Wright, P. T. May, and M. T. Decker, 1990: GAPEX: A ground-based atmospheric profiling experiment. *Bull. Amer. Meteor. Soc.,* **71,** 310–318.

Stankov, B. B., E. R. Westwater, J. B. Snider, and R. L. Weber, 1990: Remote sensor observations during WISP90: The use of microwave radiometers, RASS, and ceilometers for detection of aircraft icing conditions. NOAA Tech. Memo. ERL WPL-187, NOAA Wave Propagation Laboratory, Boulder, CO, 77 pp.

Starr, D. O., and S. H. Melfi, 1991: The Role of Water Vapor in Climate, A Strategic Research Plan for the Proposed GEWEX Water Vapor Project (GVaP). NASA Conf. Publication 3120. 50 pp.

Vane, G., (ed.), 1987: *Airborne Visible/Infrared Imaging Spectrometer* (AVIRIS). Jet Propulsion Laboratory, 73–87.

Wade, C. G., and D. E. Wolfe, 1989: Performance of the VIZ carbon hygristor in a dry environment. Proc., *12th Conf. on Weather Analysis and Forecasting,* Amer. Meteor. Soc., Monterey, 58–62.

Westwater, E. R., and J. B. Snider, 1989: Applications of ground-based radiometric observations of millimeter wave radiation. *Alta Frequenza.,* **LVIII,** 31–38.